Soft x-ray photoelectron spectroscopy of $(HfO_2)_x(SiO_2)_{1-x}$ high-k gate-dielectric structures

M. D. Ulrich,[a] J. G. Hong, J. E. Rowe, and G. Lucovsky
Department of Physics, North Carolina State University, Raleigh, North Carolina 27695-7518

A. S.-Y. Chan and T. E. Madey
Department of Physics and Astronomy and Laboratory for Surface Modification, Rutgers University, Piscataway, New Jersey 08855-0849

(Received 13 March 2003; accepted 9 May 2003; published 5 August 2003)

Soft x-ray photoelectron spectroscopy has been used to study several $(HfO_2)_x(SiO_2)_{1-x}$ film compositions. The relationships between composition and Si $2p$ and Hf $4f$ core level binding energies were investigated using nominally thick films. Both the Si $2p$ $[Si^{4+}]$ and Hf $4f$ features shift to lower binding energy by approximately 1.3 eV as the composition is varied from SiO_2 to HfO_2. The shift to lower binding energy is consistent with both an electron transfer model of the chemical environment and final-state core-hole screening resulting from differences in material polarizability. In addition, the Gaussian widths of the core levels narrow with increasing HfO_2 content. Calculations of phonon broadening indicate that this trend is due instead to inhomogeneous disorder. The dielectric/Si interface was investigated with ultrathin ($\sim$10–20 Å) films. There was virtually no difference in binding energies or Gaussian width among the various compositions, indicating a preferential composition of approximately $x=0.5$ at the interface. Interface suboxides were also investigated and indicate a quality entropy-driven oxide/silicon interface. © *2003 American Vacuum Society.* [DOI: 10.1116/1.1589518]

I. INTRODUCTION

Near-future downscaling of field-effect transistors (FETs) requires the replacement of the SiO_2 gate oxide with a material having a larger dielectric constant.[1,2] This is necessary to improve reliability and reduce tunneling current for nanometer device scaling. An obstacle in this effort is the formation of an interface between the alternative dielectric and the silicon substrate that is free of SiO_2 and does not degrade FET performance by, for example, reducing channel mobility or trapping charge. Two promising material systems that have received considerable attention are $(HfO_2)_x(SiO_2)_{1-x}$[3–12] and $(ZrO_2)_x(SiO_2)_{1-x}$.[4,6,9,10,12–18] It has been mentioned that HfO_2 based oxides are better suited for the replacement than ZrO_2 based oxides based on thermodynamic studies[9] and band gap measurements.[10]

The advantages of soft x-ray photoelectron spectroscopy (SXPS) using synchrotron radiation for characterizing an interface are high resolution, a tunable photon source with high photon flux and a short electron attenuation length which provides greater depth sensitivity. For an oxide interface with silicon, SXPS is particularly suitable because the resolution is sufficient to resolve and distinguish the suboxide states Si^{1+}, Si^{2+}, and Si^{3+} from the substrate and fully oxidized SiO_2 in the Si $2p_{3/2}$ single-component spectra. The model interface is the SiO_2/Si interface and this has been studied in detail with SXPS.[19–23] When considering an alloy with SiO_2 such as $(HfO_2)_x(SiO_2)_{1-x}$, however, the Si $2p$ Si^{4+} binding energy is less than for pure SiO_2 and the Si^{2+} and Si^{3+} oxidation states can be obscured.

This article presents SXPS studies of the Si $2p$ and Hf $4f$ core levels for several compositions of $(HfO_2)_x(SiO_2)_{1-x}$ alloys and for pure SiO_2 and HfO_2. Examining nominally thick films ($\sim$75 Å), we determine that the binding energies of both core levels decrease by approximately 1.3 eV as the composition is varied from SiO_2 to HfO_2. This is the combined result of a chemical shift due to charge transfer and a final-state core-hole screening effect. In addition, the Gaussian widths of the Si $2p$ $[Si^{4+}]$ and Hf $4f$ peaks narrow as the composition varies from SiO_2 to HfO_2 as a result of variations in inhomogeneous disorder. We also investigated complementary ultrathin $(HfO_2)_x(SiO_2)_{1-x}$ films ($\sim$10 Å) and there is not significant variation in the core level binding energies or Gaussian widths with composition. This indicates that a preferential composition of approximately $x=0.5$ forms at the $(HfO_2)_x(SiO_2)_{1-x}$/Si(111) interface. This prevents engineering of the band offsets at the interface but relaxes constraint requirements on deposition processing.

II. EXPERIMENTAL DETAILS

A. Sample preparation

Samples were prepared from either Si (111) or Ge (111) substrates. Germanium was not found to be incorporated into the oxide during deposition and results appear to be independent of substrate though this was not thoroughly investigated. Ultrathin oxide films ($\sim$10 Å) were deposited only on Si (111) substrates. H-terminated Si (111) was prepared by etching with (50:1) HF and removing the remaining oxide using 40% NH_4F. Ge (111) substrates were prepared by dipping in 1% bromine methanol for 2 min followed by a methanol rinse, a rinse in 60–90 °C de-ionized water, 2 min

[a]Author to whom correspondence should be addressed; electronic mail: mdulrich@unity.ncsu.edu

in ammonium hydroxide, another de-ionized water rinse and dried with nitrogen immediately before loading into the process system. Oxide films were grown using remote plasma enhanced chemical vapor deposition (RPECVD) at North Carolina State University using hafnium tert-butoxide held at 20 °C and 2% silane in helium as sources of hafnium and silicon. These species were introduced into the process chamber through injectors using helium as a carrier gas. The flow rates of the sources were chosen empirically to provide the target oxide composition. Oxygen is supplied separately and excited with a 13.56 MHz radio frequency plasma, at a power of 30 W. The process chamber pressure was maintained at 0.3 Torr and the substrate temperature was maintained at 200 °C during deposition. The deposition times were chosen to result in approximately 75 Å for the thick films and 10 Å for the ultrathin films. After deposition, the alloy composition was determined by comparing Hf and Si peak intensities from on-line Auger electron spectroscopy which is calibrated against Rutherford backscattering spectrometry. Thick $(HfO_2)_x(SiO_2)_{1-x}$ films were grown with compositions of $x=0$, 0.25 ± 0.05, 0.50 ± 0.05, 0.85 ± 0.05 and 1.0. Ultrathin films were grown with compositions of $x=0.25\pm0.05$, 0.50 ± 0.05, 0.75 ± 0.05, and 1.0. The thick films were measured as deposited. *In situ* annealing studies of thick films showed no significant change in SXPS data after heating up to 900 °C. Ultrathin films were annealed at 500 °C for 30 s by rapid thermal annealing similar to earlier studies of $(Ta_2O_5)_x(Al_2O_3)_{1-x}$ alloys.[24] The temperature was chosen to be well below the crystallization temperature of HfO_2.

B. SXPS measurements

Samples were transported from the RPECVD process chamber at North Carolina State University to the U4A beamline of the National Synchrotron Light Source in a nitrogen atmosphere to minimize exposure to air. Some exposure, generally several hours, was unavoidable during the transfer and mounting of samples. The U4A beamline includes a 6 m spherical grating monochromator that produces photons between 10 and 250 eV. Data were obtained at photon energies of 130 and 170 eV. The instrumental resolutions at these photon energies were approximately 0.2 and 0.5 eV. Photoelectrons were detected with a VSW 100 mm hemispherical analyzer fixed at 45° relative to the photon beam axis. Measurements were taken at normal takeoff.

The Si $2p_{3/2}$ single-component spectra presented in this article were extracted from the raw data using a standard spin-orbit stripping procedure with a spin-orbit energy splitting of 0.602 eV and a branching ratio of 2:1. For the thick films, only the Si^{4+} oxidation state was detectable and was fit with a single Voigt function peak. For the ultrathin films, the oxide, substrate and interface suboxide states were detectable. The substrate binding energy relative to the Fermi level was determined to be 99.41 ± 0.02 eV. In most cases, the Si^{3+} state was not resolved due to the much more intense Si^{4+} core level. To retain a physically relevant model of the data, relationships between the suboxide states and substrate known from previous studies of the SiO_2/Si interface[23] were used to constrain the fits, minimizing the number of free parameters. These relationships were the relative intensities, binding energies, and peak widths.

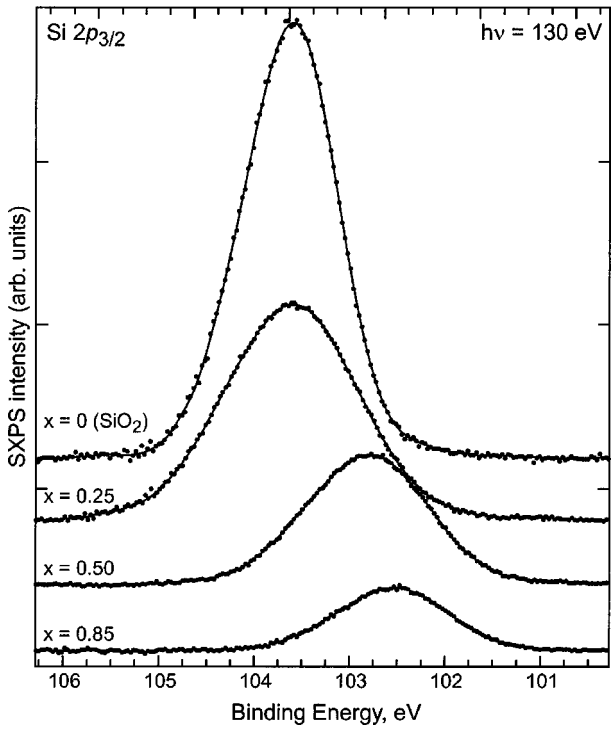

FIG. 1. Si $2p_{3/2}$ single-component spectra for nominally thick films of SiO_2 and $(HfO_2)_x(SiO_2)_{1-x}$ alloys with $x=25\%$, 50%, and 85%. The spectra are normalized to the photon flux. The data were taken with a photon energy of 130 eV.

Because of the relatively low Hf $4f_{7/2}$ binding energy (~18 eV), overlap with the valence band complicated the fitting of the Hf $4f$ core level spectra. For the ultrathin films, the background was fit using the equation $a+bx+cx^d$. For the thick films, the O $2s$ and O $2p$ signals to either side of the Hf $4f$ core level were stronger and were modeled with broad Gaussian peaks. The valence band structure directly underneath the Hf $4f$ core level features was determined to have a negative slope and negative concavity by comparing the HfO_2 valence band with the valence bands of SiO_2 and ZrO_2 films with similar thickness. Two Voigt function peaks were used to fit the Hf $4f$ peak pair. For the thin film data, the Lorentzian full width at half maximum varied between 100 and 200 meV with an average of 144 meV. The average energy splitting was 1.67 eV and the average branching ratio was 0.75. For the thick films, the Lorentzian full width at half maximum was fixed at 42 meV. The average energy splitting was 1.66 eV and the average branching ratio 0.75.

III. RESULTS

A. Thick film results

Figure 1 shows the Si $2p_{3/2}$ single-component spectra for SiO_2 and for alloys having 25%, 50%, and 85% HfO_2 content. These data were taken at a photon energy of 130 eV and

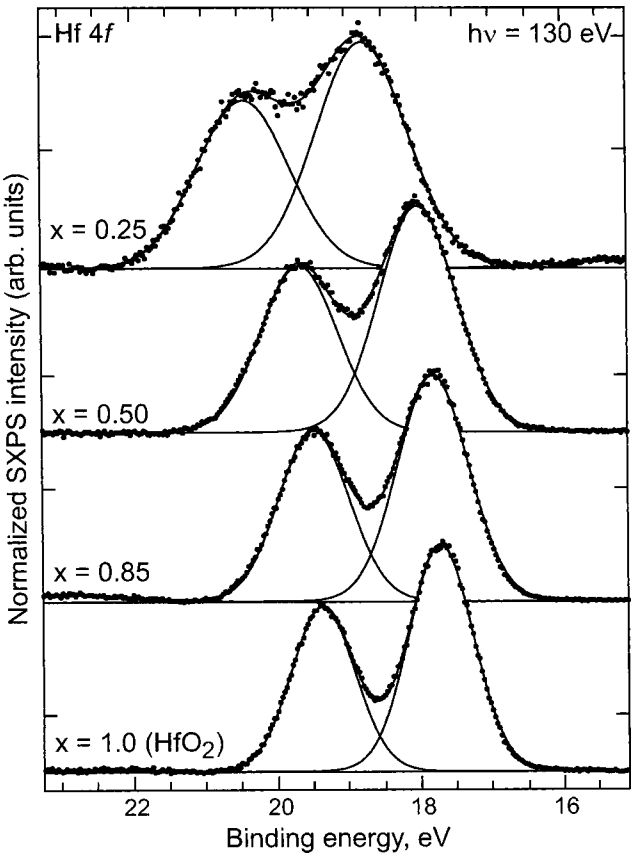

FIG. 2. Hf $4f$ spectra for nominally thick films of $(HfO_2)_x(SiO_2)_{1-x}$ alloys with $x=25\%$, 50%, 85%, and 100% (HfO_2). The spectra are normalized to the Hf $4f_{7/2}$ peak height. The data were taken with a photon energy is 130 eV.

normalized to the photon flux. Only the Si^{4+} oxidation state is detectable indicating that the film is thicker than 30 Å. The intensity of the Si^{4+} peak scales with composition. The binding energy of this core level shifts from 103.63 eV for SiO_2 to 102.55 eV for $(HfO_2)_{0.85}(SiO_2)_{0.15}$. The Gaussian widths of the three alloys, after correcting for the theoretical instrumental resolution, are broader than that of pure SiO_2, and decrease with increasing HfO_2 content for the alloys. Figure 2 shows the corresponding Hf $4f$ spectra for the samples having 25%, 50%, 85%, and 100% HfO_2 composition. These data were also taken at a photon energy of 130 eV. The spectra have been normalized to the Hf $4f_{7/2}$ peak intensity which does not scale with composition as discussed later in the article. The binding energy of the Hf $4f_{7/2}$ core level shifts from 18.75 eV for $(HfO_2)_{0.25}(SiO_2)_{0.75}$ to 17.71 eV for pure HfO_2. The Gaussian width of each of the Hf $4f$ peaks, after correcting for the theoretical instrumental resolution, monotonically decreases from 1.45 eV for $(HfO_2)_{0.25}(SiO_2)_{0.75}$ to 1.01 eV for pure HfO_2. The binding energies and Gaussian widths of the Si $2p_{3/2}$ and Hf $4f_{7/2}$ core levels are summarized in Table I.

B. Ultrathin film results

Figure 3 compares the Si $2p_{3/2}$ single-component spectra for samples having a HfO_2 composition of 25%, 50%, 75%, and 100%. The data were taken with a photon energy of 170 eV to enhance sensitivity to the substrate and interface states. The spectra are normalized to the substrate (Si^0) peak height and aligned to the Si^0 peak at a binding energy of 99.41 eV with respect to the Fermi level. The three suboxide interface states, Si^{1+}, Si^{2+}, and Si^{3+} are shown as dashed lines. The intensity ratio of the Si^{4+} and Si^0 peaks is lower for the SiO_2-rich samples than it is for the HfO_2 and HfO_2-rich samples. The Si^{4+} binding energy and peak width are virtually the same for all samples indicating a preferential composition for these films. The average binding energy is 102.89 eV and varies by only 0.15 eV. The pure HfO_2

TABLE I. Summary of binding energies and peak widths for thick $(HfO_2)_x(SiO_2)_{1-x}$ films. The theoretical instrumental resolution has been subtracted from the peak widths.

	Si $2p_{3/2}$ [Si^{4+}]		Hf $4f_{7/2}$	
x	BE	Width	BE	Width
1.0 (HfO_2)	⋯	⋯	17.71 eV	1.01 eV
0.85	102.55 eV	1.24 eV	17.81 eV	1.10 eV
0.50	102.80 eV	1.36 eV	18.00 eV	1.22 eV
0.25	103.62 eV	1.49 eV	18.75 eV	1.45 eV
0.0 (SiO_2)	103.63 eV	1.06 eV	⋯	⋯

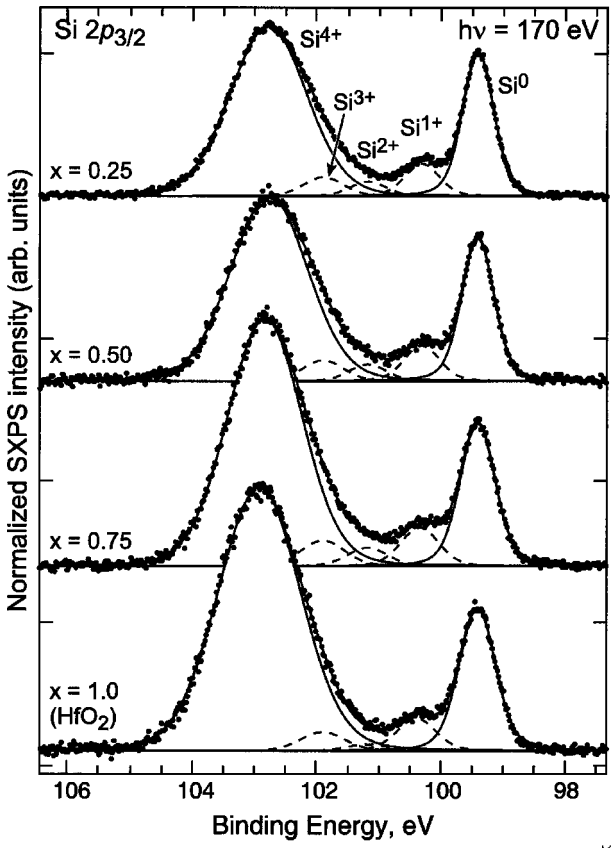

FIG. 3. Si $2p_{3/2}$ single-component spectra for ultrathin films of $(HfO_2)_x(SiO_2)_{1-x}$ alloys with $x=25\%$, 50%, 75%, and 100% (HfO_2). The spectra are normalized to the substrate (Si^0) peak height and aligned to the substrate peak position which averaged 99.41 eV. The data were taken with a photon energy of 170 eV.

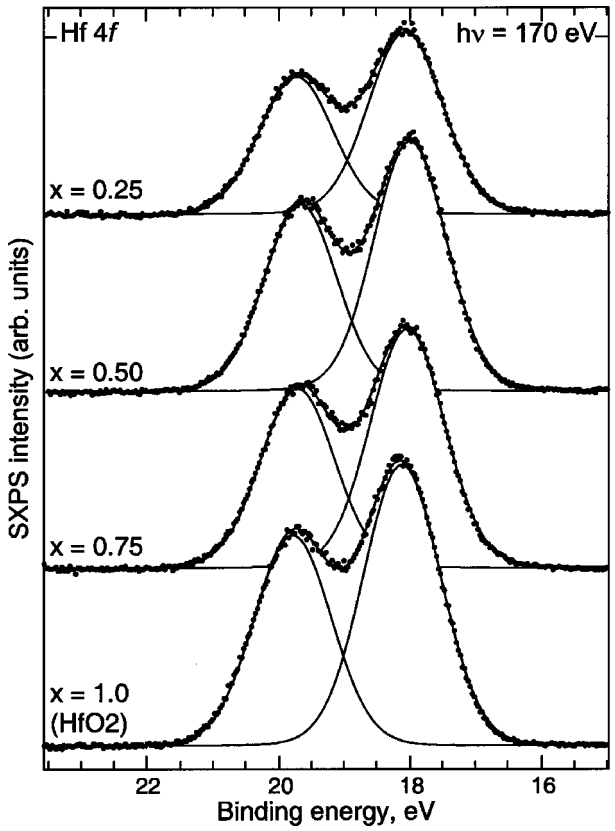

FIG. 4. Hf $4f$ spectra for ultrathin films of $(HfO_2)_x(SiO_2)_{1-x}$ alloys with $x=25\%$, 50%, 75%, and 100% (HfO_2). The spectra are normalized to the photon flux. The data were taken with a photon energy of 170 eV.

sample has a binding energy of 102.97 eV which is slightly higher than the average. The Si^{4+} peak width is the same for all thin film samples, averaging 1.26 eV after correcting for the theoretical instrumental resolution and varying by only 0.05 eV.

For all samples, the relationships between the interface peaks and substrate peak for the $SiO_2/Si(111)$ were used to minimize the number of free parameters in the fitting procedure. Parameters were relaxed as necessary to obtain a statistically satisfactory fit. For the intended alloy depositions, the suboxide states indicated a quality entropy-driven interface typical of $SiO_2/Si(111)$ interfaces annealed at moderate temperatures (below 700 °C).[23] The intended HfO_2 deposition, however, had a much lower Si^{2+} intensity which would be expected for $SiO_2/Si(111)$ interfaces annealed above 800 °C.[23] In all cases the suboxide states indicate quality interfaces that are similar to those of device-grade $SiO_2/Si(111)$ interfaces.

Figure 4 shows the corresponding Hf $4f$ spectra. The photon energy was 170 eV and the instrumental resolution 0.5 eV. The spectra are normalized to the photon flux. The Hf $4f$ intensity of the $x=0.75$ and $x=0.50$ samples is 15% less than the $x=1.0$ sample and for the $x=0.25$ sample is 35% less than the $x=1.0$ sample. The Hf $4f_{7/2}$ binding energy is virtually the same among the samples averaging 18.08 eV and varying by 0.18 eV. The binding energy of the HfO_2 sample is 18.17 eV which is slightly higher than the alloys.

TABLE II. Summary of binding energies and peak widths for ultrathin $(HfO_2)_x(SiO_2)_{1-x}$ films. The theoretical instrumental resolution has been subtracted from the peak widths.

	Si $2p_{3/2}$ [Si^{4+}]		Hf $4f_{7/2}$	
x	BE	Width	BE	Width
1.0 (HfO_2)	102.97 eV	1.28 eV	18.17 eV	1.24 eV
0.75	102.87 eV	1.23 eV	18.08 eV	1.16 eV
0.50	102.82 eV	1.24 eV	17.99 eV	1.14 eV
0.25	102.85 eV	1.27 eV	18.06 eV	1.17 eV
0.0 (SiO_2)	⋯	⋯	⋯	⋯

The peak width is also virtually the same, averaging 1.18 eV after correcting for the theoretical instrumental resolution and varying only by 0.1 eV. The width of the HfO_2 sample is 1.24 eV which is slightly broader than the alloy samples. The binding energies and Gaussian widths of the Si $2p_{3/2}$ and Hf $4f_{7/2}$ core levels are summarized in Table II.

The binding energies for both the thick and thin samples are plotted as a function of the alloy composition in Fig. 5. Figure 5(a) shows the Si $2p$ [Si^{4+}] binding energy and Fig. 5(b) shows the Hf $4f_{7/2}$ binding energy. The lines are provided as a guide to the eye. In both core levels, the binding

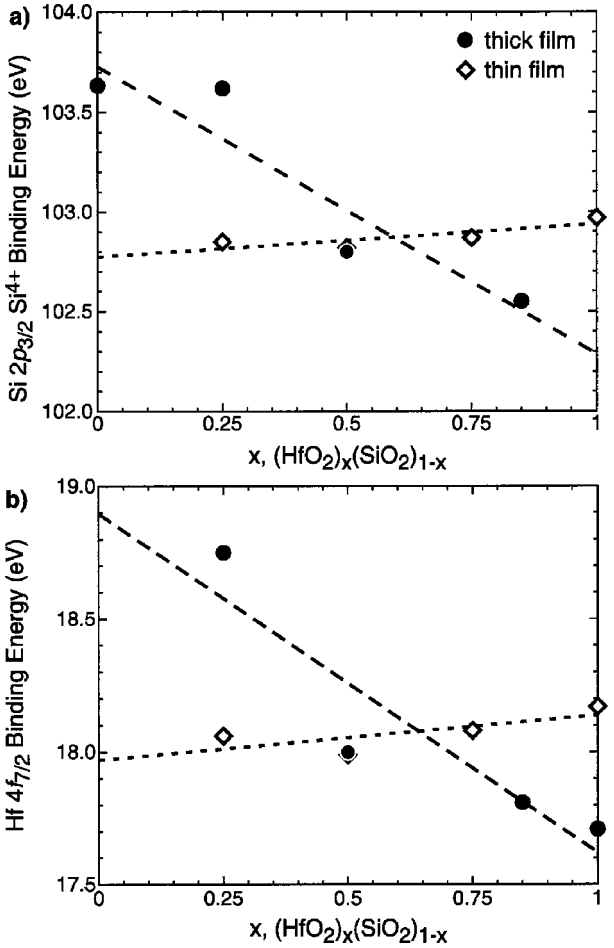

FIG. 5. Si $2p_{3/2}$ Si^{4+} (a) and Hf $4f_{7/2}$ (b) binding energies of thick (●) and thin (◇) film samples as a function of alloy composition. The lines are provided as a guide to the eye.

energies in the thick film samples reduce by about 1.3 ± 0.2 eV as the composition varies from SiO_2 to HfO_2. The binding energies in the thin films are insignificantly different except for the pure HfO_2 for which the binding energies are approximately 0.1 eV higher.

IV. DISCUSSION

A. Thick films

The 1.3 eV shift in the binding energies as composition varies from SiO_2 to HfO_2 is in agreement with other studies of this material system.[4,6,10] The chemically similar $(ZrO_2)_x(SiO_2)_{1-x}$ system also exhibits a similar trend.[6,10,14] The direction of the shift is consistent with an electron-transfer model and with differences in final-state core-hole screening among the samples. Consider first the chemical environment. The electronegativities of Si, Hf and O are 1.9, 1.3 and 3.5, respectively.[25] Because Hf has a lower electronegativity than Si, Hf–O bonds are more ionic than Si–O bonds. Due to second neighbors in the alloy, however, Hf–O and Si–O bonds are less ionic in HfO_2-rich alloys than in SiO_2-rich alloys resulting in lower binding energies for HfO_2-rich $(HfO_2)_x(SiO_2)_{1-x}$ alloys. A calculation of the effective charge on each atom as a function of the composition clearly illustrates this and has been reported for the chemically similar $(ZrO_2)_x(SiO_2)_{1-x}$ system.[14] This result is consistent with previous explanations of core level shifts in oxide alloys.[6,14,15,26] Now consider the final-state core-hole screening effect. At optical frequencies, corresponding to the time scale of the photoemission process, HfO_2 has a dielectric constant of 4.0[27] and SiO_2 has a dielectric constant of 2.1.[28] Thus core-hole screening is increased with increasing HfO_2 composition and core level binding energies decrease correspondingly. There are conflicting reports as to which of these two effects dominates. Guittet and co-workers, using density functional theory to determine ionicity in $ZrSiO_4$, ZrO_2 and SiO_2, and taking into account relaxation effects, concluded that the leading contribution is from the charge transfer.[15] However, Opila and co-workers mention that if charge transfer effects, which are localized, were primarily responsible for the shift, probable local compositional inhomogeneities would be revealed as broader peaks. In the final state, however, effects are long range and would average out inhomogeneities. Based on this and x-ray absorption spectroscopy they conclude that the final state must provide the greatest contribution to the shift.[6] We have not estimated which of these two effects dominates the core level shifts.

The reported shift in the core level binding energies for $(ZrO_2)_x(SiO_2)_{1-x}$ is 1.8 eV, approximately 40% larger than measured here for $(HfO_2)_x(SiO_2)_{1-x}$.[14] The electronegativities of Hf and Zr are virtually identical (1.3 for Hf and 1.4 for Zr)[25] as are the dielectric constants of their oxides. This indicates that the difference in core level shifts is not due to the effects mentioned above. A possible explanation may be variations in electron density that might arise from fundamental differences in binding through $4d$ orbitals (for Zr–O bonds) and binding through $5d$ orbitals (for Hf–O bonds).

All thick samples, with the exception of the pure SiO_2, show a narrowing of the Si $2p$ and Hf $4f$ core levels with increasing HfO_2 content (see Table I). There are three contributions to the Gaussian width of core levels in photoemission: the instrumental width, phonon broadening, and inhomogeneous disorder. The instrumental width is the same for these measurements. To determine if the trend in the Gaussian width is due to phonon broadening variations, the phonon widths for SiO_2 and HfO_2 were calculated using the theory of Iwan and Kunz.[29] Briefly, the theory states that phonon broadening is related to the square root of the average longitudinal optical phonon energy and the relaxation energy of the excited (ionized) state of the core level. For the calculation, static dielectric constants of 20 and 3.8 and dynamic dielectric constants of 4.0[27] and 2.1[28] were used for HfO_2 and SiO_2, respectively. Fourier transform infrared spectroscopy data which provide a measure of the transverse optical phonons was used in conjunction with the Lyddane–Sychs–Teller relationship[30] to estimate an average longitudinal optical phonon energy. We found that while the average longitudinal optical phonon energy is significantly larger for SiO_2, the relaxation energy of the excited state of the core level is lower. Thus the theoretical phonon broadening of the core levels is essentially the same for HfO_2 and SiO_2. We conclude then that the differences in Gaussian width among the different compositions must be due to inhomogeneous disorder. The practical value of understanding the peak width is that broad peaks do not necessarily indicate separate phases as might be anticipated when measuring ultrathin films.

It is intuitive that one should be able to determine the alloy composition from the ratio of the core level intensities of the alloys to those of the binary oxides. For data taken at a photon energy of 130 eV, this was the case with the Si $2p$ peaks but was not the case with the Hf $4f$ peaks. Most dramatically, the Hf $4f$ intensity of the $(HfO_2)_{0.85}(SiO_2)_{0.15}$ film was nearly three times that of the pure HfO_2 film. Nor were other compositions commensurate with the intensity ratios. At a photon energy of 130 eV, the kinetic energy of Si $2p$ photoelectrons is $\sim$20 eV whereas the kinetic energy of Hf $4f$ photoelectrons is $\sim$110 eV. This effect was examined as a function of the photoelectron kinetic energy with a second set of samples. At lower kinetic energy of Hf $4f$ photoelectrons, the Hf $4f$ intensity does follow the composition. This may indicate a compositional difference between the bulk and surface of the deposited films. It may also arise from other possible mechanisms such as differences in density, local ordering at the surface leading to photoelectron diffraction or nonuniform water absorption in the film.

B. Ultrathin films

Remarkably, the composition of these ultrathin films was independent of the deposition conditions. This conclusion is based on two results. First, the Si $2p_{3/2}$ $[Si^{4+}]$ and Hf $4f_{7/2}$ binding energies for all four ultrathin films correspond to a thick film composition of approximately $(HfO_2)_{0.6}(SiO_2)_{0.4}$ (see Fig. 5.) Second, the Si $2p_{3/2}$ $[Si^{4+}]$ and Hf $4f_{7/2}$ peak

widths are narrow (compare Tables I and II) and similar among the films. This indicates a single alloy composition and the absence of significant SiO_2 at the interface. In estimating this composition, comparisons of the binding energies with thick film results must be considered carefully. Final-state core-hole screening from adjacent materials (particularly the Si substrate) plays a significant role in the measured binding energy of Si $2p$ $[Si^{4+}]$ for ultrathin SiO_2 films (<20 Å) on Si.[22,23,31,32] This can reduce the measured binding energy from that of bulk SiO_2 by as much as 0.5 eV. The ultrathin films in this study are estimated to be 14–16 Å based on the ratio of the Si^{4+} to Si^0 peak intensities. Because of this effect, the initial-state binding energy is likely to be somewhat higher for both the Si $2p$ $[Si^{4+}]$ and Hf $4f$ core levels, and the composition is likely to be roughly $(HfO_2)_{0.5}(SiO_2)_{0.5}$. Note that this core-hole screening from adjacent materials is in addition to the screening caused by the oxide itself.

V. CONCLUSION

We have shown that the Si $2p$ and Hf $4f$ binding energies reduce by roughly 1.3 eV as $(HfO_2)_x(SiO_2)_{1-x}$ composition is varied from SiO_2 to HfO_2. This shift is due in part to changes in the bonding environment and in part to differences in final-state core-hole screening. The relationship between Hf $4f$ peak intensity, composition and photon energy is not understood at this time. The most notable conclusion is that the interface is driven to a specific composition regardless of the deposition conditions. This indicates that the band offsets at the silicon interface are fixed and cannot be engineered by choosing the composition. This allows for little control over the interface but eases FET processing constraints. Also encouraging is the result that we do not find pure SiO_2 at the interface but an acceptable alloy composition. Investigation of the Si suboxide states also reveals that the suboxide interface is of comparable quality to the $SiO_2/Si(111)$ interface.

[1]*International Roadmap for Semiconductors* (Semiconductor Industry Association, San Jose, CA, 2001); http://public.itrs.net/
[2]G. D. Wilk, R. M. Wallace, and J. M. Anthony, J. Appl. Phys. **89**, 5243 (2001).
[3]G. D. Wilk and R. M. Wallace, Appl. Phys. Lett. **74**, 2854 (1999).
[4]G. D. Wilk, R. M. Wallace, and J. M. Anthony, J. Appl. Phys. **87**, 484 (2000).
[5]A. Callegari, E. Cartier, M. Gribelyuk, H. F. Okorn-Schmidt, and T. Zabel, J. Appl. Phys. **90**, 6466 (2001).
[6]R. L. Opila, G. D. Wilk, M. A. Alam, B. van Dover, and B. M. Busch, Appl. Phys. Lett. **81**, 1788 (2002).
[7]O. Renault, D. Samour, J.-F. Damlencourt, D. Blin, F. Martin, S. Marthon, N. T. Barrett, and P. Besson, Appl. Phys. Lett. **81**, 3627 (2002).
[8]H. Kang, Y. Roh, G. Bae, D. Jung, and C.-W. Yang, J. Vac. Sci. Technol. B **20**, 1360 (2002).
[9]M. Gutowski, J. E. Jaffe, C.-L. Liu, M. Stoker, R. I. Hegde, R. S. Rai, and P. J. Tobin, Appl. Phys. Lett. **80**, 1897 (2002).
[10]H. Kato, T. Nango, T. Miyagawa, T. Katagiri, K. S. Seol, and Y. Ohki, J. Appl. Phys. **92**, 1106 (2002).
[11]M. A. Quevedo-Lopez, M. El-Bouanani, M. J. Kim, B. E. Gnade, R. M. Wallace, M. R. Visokay, M. Douglas, M. J. Bevan, and L. Colombo, Appl. Phys. Lett. **81**, 1609 (2002).
[12]M. A. Quevedo-Lopez, M. El-Bouanani, B. E. Gnade, R. M. Wallace, M. R. Visokay, M. Douglas, M. J. Bevan, and L. Colombo, J. Appl. Phys. **92**, 3540 (2002).
[13]D. A. Muller and G. D. Wilk, Appl. Phys. Lett. **79**, 4195 (2001).
[14]G. B. Rayner, Jr., D. Kang, Y. Zhang, and G. Lucovsky, J. Vac. Sci. Technol. B **20**, 1748 (2002).
[15]M. J. Guittet, J. P. Crocombette, and M. Gautier-Soyer, Phys. Rev. B **63**, 125117 (2001).
[16]H. Kim and P. C. McIntyre, J. Appl. Phys. **92**, 5094 (2002).
[17]F. Giustino, A. Bongiorno, and A. Pasquarello, Appl. Phys. Lett. **81**, 4233 (2002).
[18]G.-M. Rignanese, F. Detraux, X. Gonze, A. Bongiorno, and A. Pasquarello, Phys. Rev. Lett. **89**, 117601 (2002).
[19]F. J. Himpsel, F. R. McFreely, A. Taleb-Ibrahimi, J. A. Yarmoff, and G. Hollinger, Phys. Rev. B **38**, 6084 (1988).
[20]Z. H. Lu, M. J. Graham, D. T. Jiang, and K. H. Tan, Appl. Phys. Lett. **63**, 2941 (1993).
[21]F. Rochet, Ch. Poncey, G. Dufour, H. Roulet, C. Guillot, and F. Sirotti, J. Non-Cryst. Solids **216**, 148 (1997).
[22]K. Z. Zhang, J. N. Greeley, M. M. Banaszak Holl, and F. R. McFeely, J. Appl. Phys. **82**, 2298 (1997).
[23]J. W. Keister, J. E. Rowe, J. J. Kolodziej, H. Niimi, H.-S. Tao, T. E. Madey, and G. Lucovsky, J. Vac. Sci. Technol. A **17**, 1250 (1999).
[24]M. D. Ulrich, R. S. Johnson, J. G. Hong, G. Lucovsky, J. S. Quinton, and T. E. Madey, J. Vac. Sci. Technol. B **20**, 1732 (2002).
[25]L. Pauling, *The Nature of the Chemical Bond and the Structure of Molecules and Crystals* (Cornell University Press, Ithaca, NY, 1960), p. 93.
[26]T. L. Barr, J. Vac. Sci. Technol. A **9**, 1793 (1991).
[27]H. A. Macleod, *Thin-Film Optical Filters*, 3rd ed. (Institute of Physics, Philadelphia, 2001), p. 623.
[28]H. R. Philipp in *Handbook of Optical Constants of Solids*, edited by E. D. Palik (Academic, Orlando, 1985), p. 760.
[29]M. Iwan and C. Kunz, Phys. Lett. **60A**, 345 (1977).
[30]C. Kittel, *Introduction to Solid State Physics*, 5th ed. (Wiley, New York, 1976), p. 306.
[31]R. Browning, M. A. Sobolewski, and C. R. Helms, Phys. Rev. B **38**, 13407 (1988).
[32]A. Pasquarello, M. S. Hybertsen, and R. Car, Phys. Rev. B **53**, 10942 (1996).